Munc18c depletion attenuates caerulein hyperstimulation induced pancreatitis

Subhankar Dolai, Tao Liang, Abrahim I. Orabi, Li Xie, Douglas Holmyard, Tanveer A. Javed, Nestor A. Fernandez, Huanli Xie, Mark S. Cattral, Debbie C. Thurmond, Peter Thorn, Herbert Y. Gaisano.

Supplementary Figure 1 (Related to Figure 1)

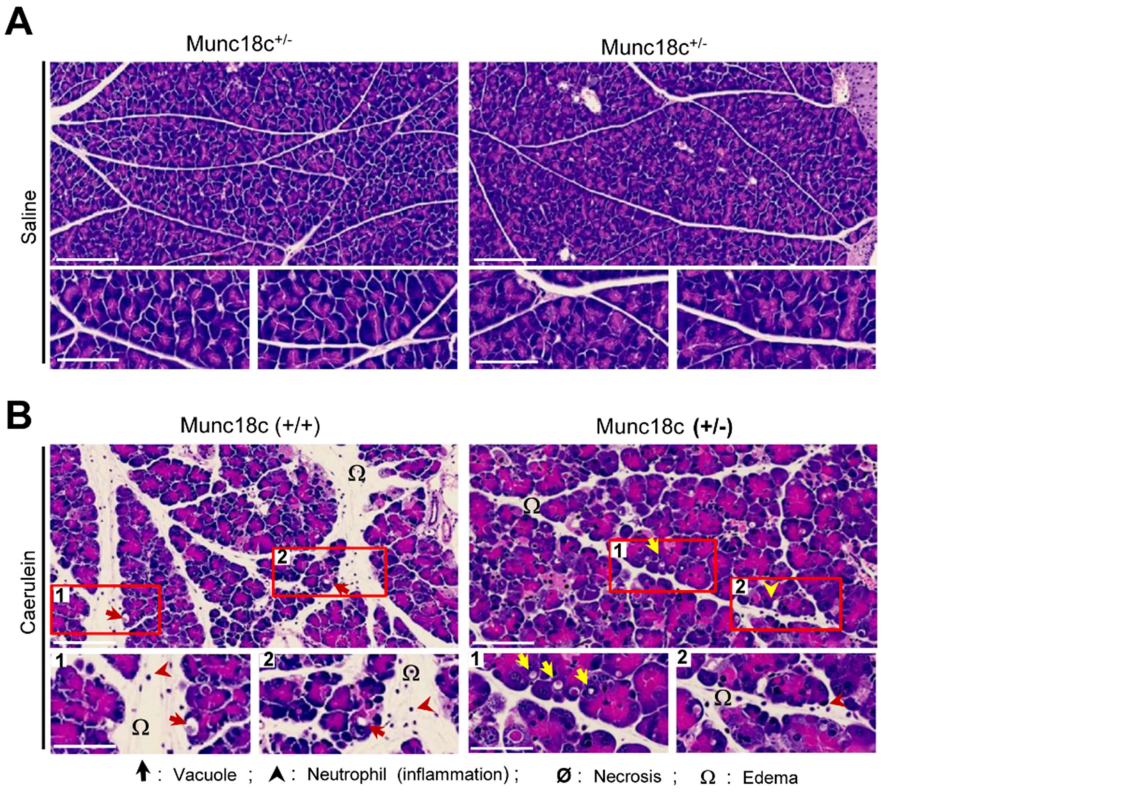

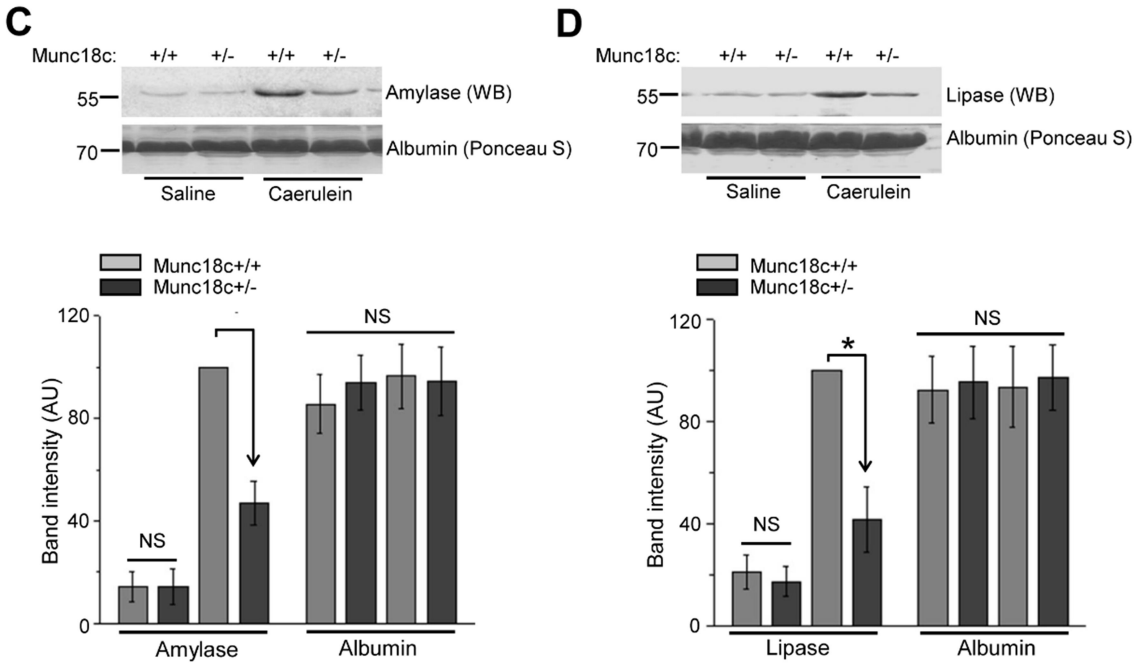

Supplementary Figure 1. (*A,B*) Related to **Fig. 1C**. Larger area of histology images with magnified regions at the bottom showing less pancreatic injury in Munc18c$^{+/-}$ mice. (*C,D*) Amylase and lipase are less abundant in the serum of caerulein administered Munc18c$^{+/-}$ mice compared to their WT littermates. 5.0 µL of serum from each of the mice that were analyzed in **Fig. 1E** were extracted (separately for each condition) and mixed thoroughly. 1.0 µL of serum mix was analyzed by Western blot (3 separate mouse samples) to detect the levels of (*C*) amylase and (*D*) lipase. Serum albumin was detected by Ponceau-S staining to monitor loading. Corresponding *bottom* graphs are densitometry analysis taking the maximum intensity band as 100. Albumin densitometry shows equal loading. Data expressed as mean ± S.D.

Supplementary Figure 2 (Related to Fig. 2B)

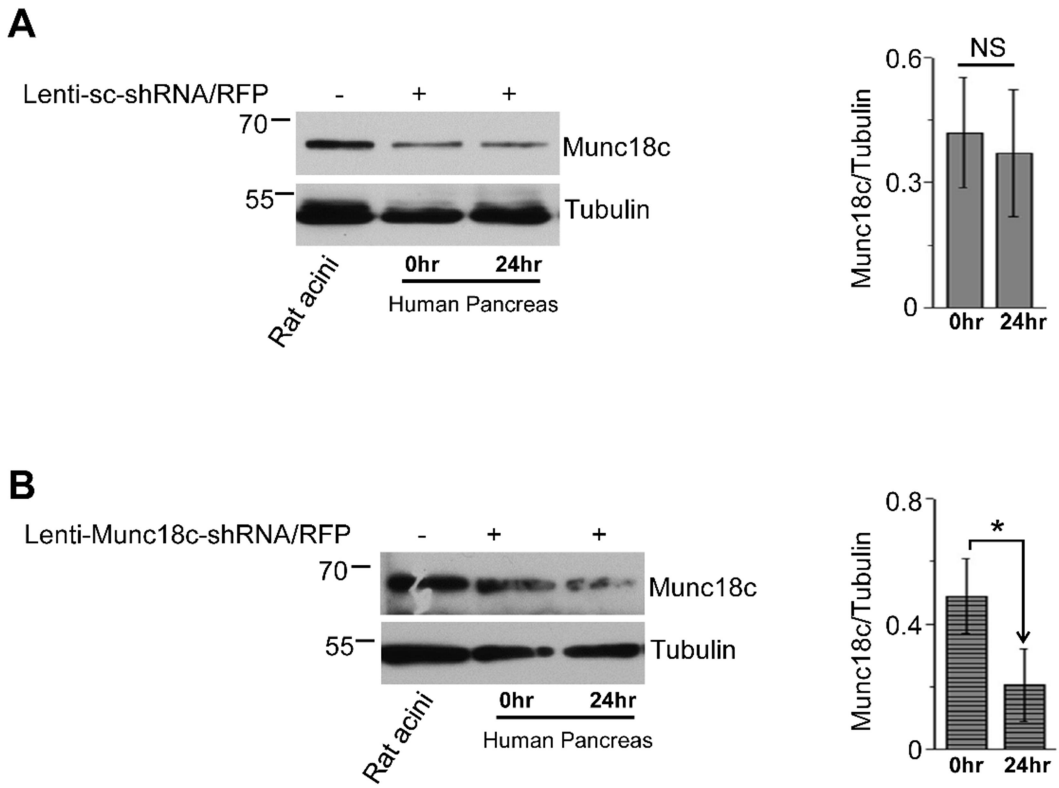

Supplementary Figure 2. Lenti-Munc18c-shRNA/RFP effectively depletes Munc18c in cultured human pancreas slices. (*A, B*) Western blot analysis of the expression of Munc18c in human pancreas slices that were transduced with either lenti-sc-shRNA/RFP (A) or lenti-Munc18c-shRNA/RFP (B) for 24 hr. Rat acini lysates were used as positive control for Munc18c. Blots shown are representative of 3 independent experiments. Analyses of band density normalized to tubulin are shown *right*. 24 hr knock-down pancreas slices were used in all human pancreas related experiments. Data expressed as ± S.D. NS=Not significant. **P*<0.05

Supplementary Figure 3

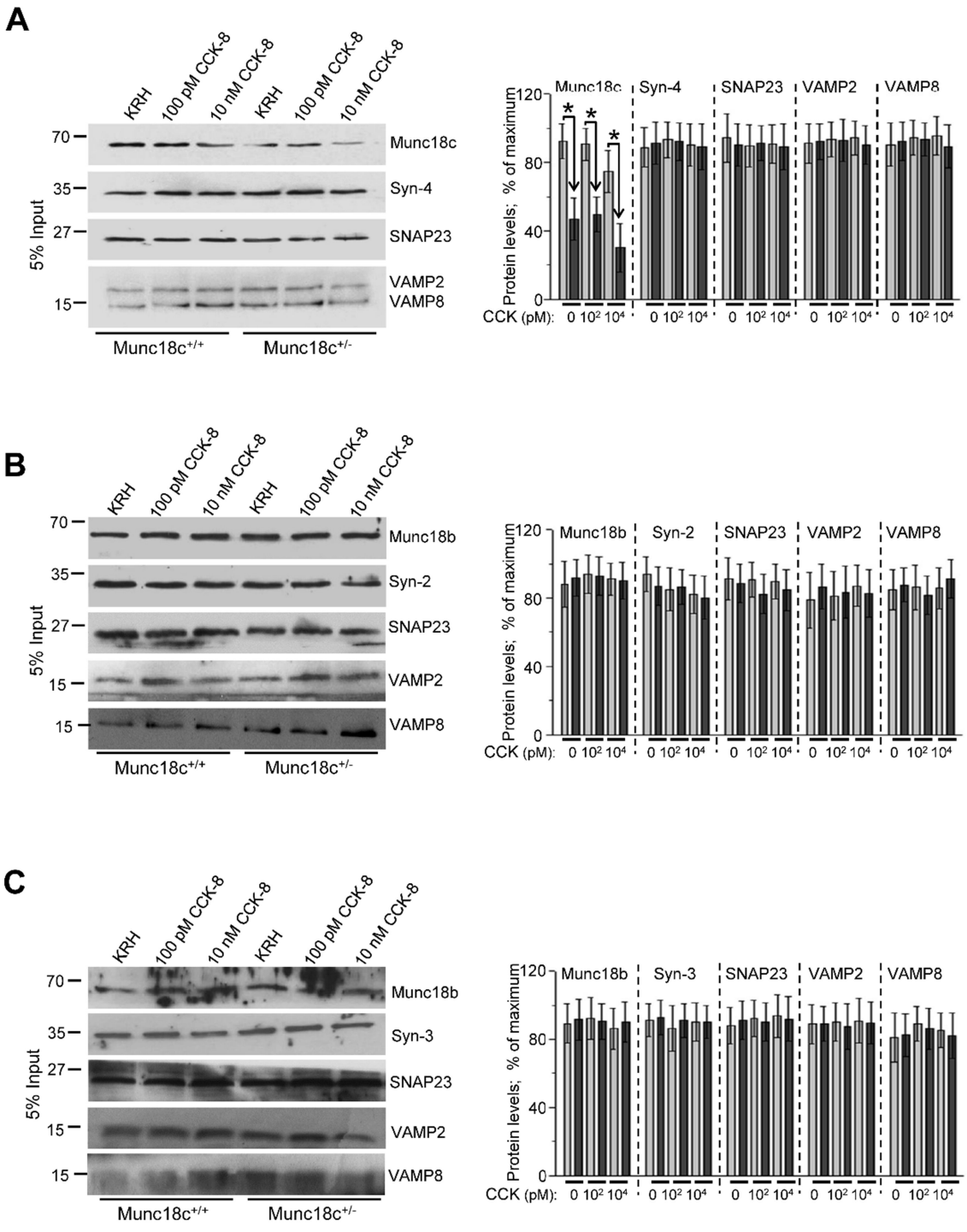

Supplementary Figure 3. Input controls correspond to Fig. 4A, Fig. 4B and Fig. 4C. (*A*, *B* and *C*) *Left panels* are the representative blots from 3 independent experiments showing 5% input controls that correspond to **Fig. 4A**, **Fig. 4B** and **Fig. 4C**. Corresponding r*ight panels* are the densitometry analysis taking the most intense band as 100 from 3 independent experiments. All proteins displayed similar level

of expression except Munc18c. In WT acini, Munc18c levels were reduced by 47% at 10 nM CCK-8 stimulation, which we previously showed was a result of displacement from the basolateral plasma membrane with subsequent cytosolic proteasomal degradation (26-29). Compared to the WT acini, Munc $18c^{+/-}$ acini displayed 52% lower expression of Munc18c in Control and 100 pM CCK-8 stimulated Munc$18c^{+/-}$ acini, with an even further reduction upon 10 nM CCK-8 stimulation. Data are presented as mean ± S.D. *P<0.05.

Supplementary Figure 4

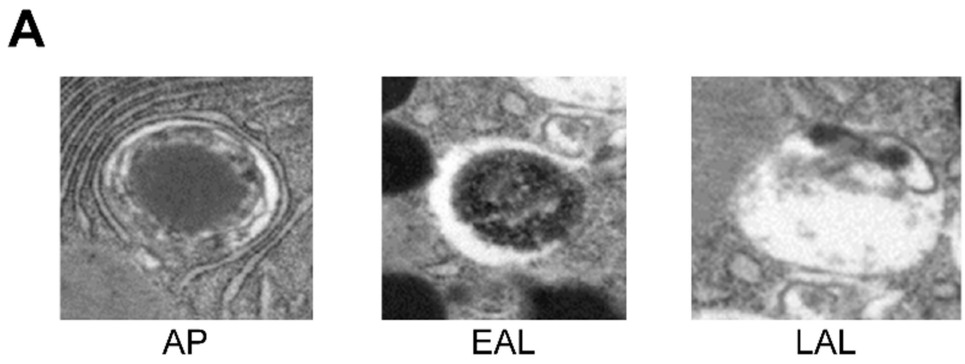

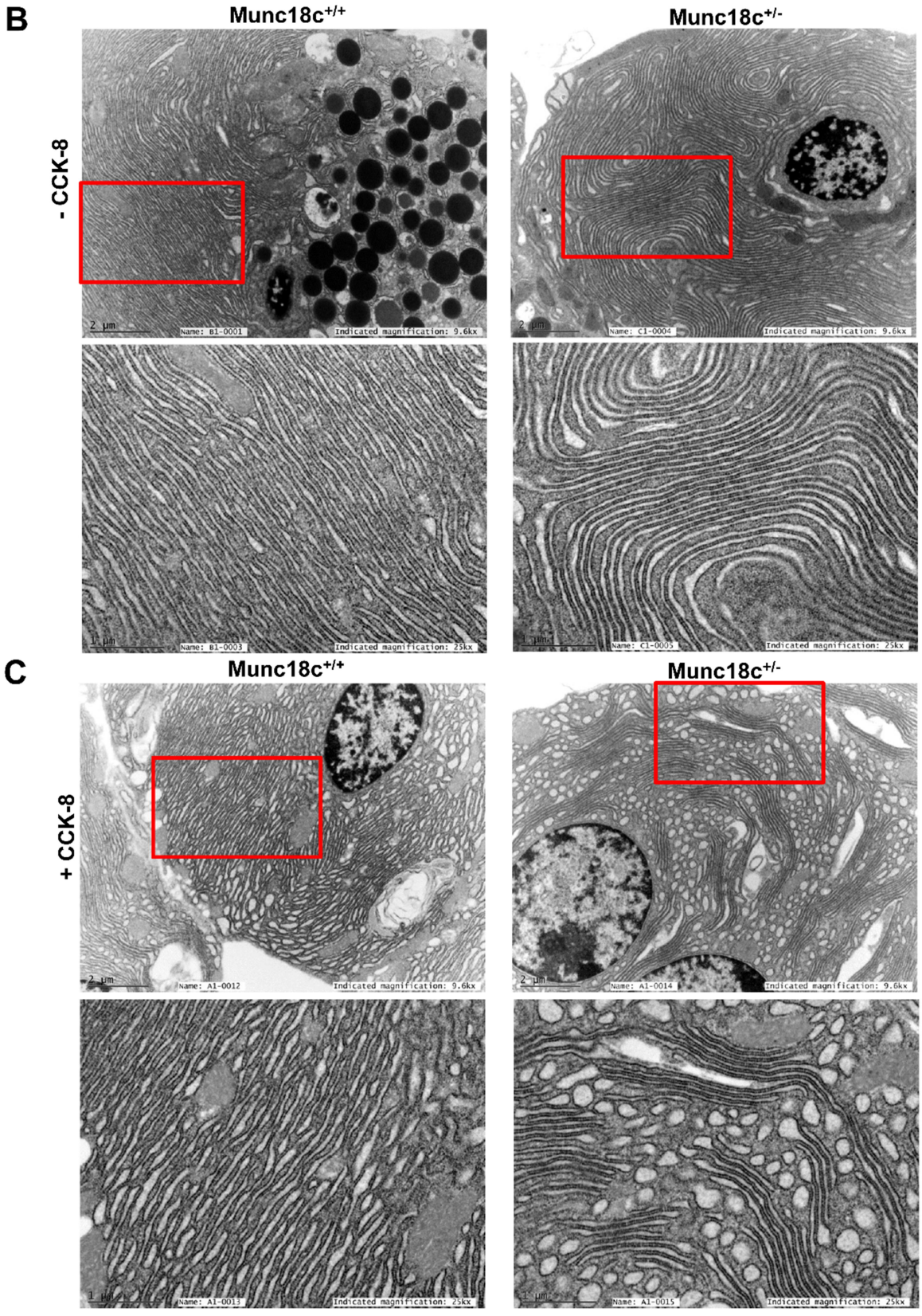
B
Munc18c+/+
Munc18c+/-
- CCK-8
2 µm
Name: B1-0001
Indicated magnification: 9.6kx
Name: C1-0004
Indicated magnification: 9.6kx
1 µm
Name: B1-0003
Indicated magnification: 25kx
Name: C1-0005
Indicated magnification: 25kx
C
Munc18c+/+
Munc18c+/-
+ CCK-8
2 µm
Name: A1-0012
Indicated magnification: 9.6kx
Name: A1-0014
Indicated magnification: 9.6kx
1 µm
Name: A1-0013
Indicated magnification: 25kx
Name: A1-0015
Indicated magnification: 25kx

Supplementary Figure 4 (Related to Fig. 5B and 5E). (*A*) Representative examples of distinct autophagy vacuole morphology, used to quantify **Fig. 5B**. *Left,* Autophagosome (AP: double membraned with undigested substances); *middle,* Early autolysosome (EAL: single membraned with undigested substances) and *right,* Late autolysosomes (LAL: single membraned with amorphous electron dense substances). (*B, C*) Additional TEM images from Control (B; -CCK) and 10 nM CCK-stimulated (C) WT (*left*) and Munc18c$^{+/-}$ (*right*) acini. Boxed areas are magnified and shown at corresponding bottom images for better views of the ER morphology. Whereas the ER appeared similar between WT and Munc18c$^{+/-}$ at the unstimulated state, after supramaximal 10 nM CCK stimulation, more and severely dilated ERs are evident in Munc18c$^{+/-}$ acinar cells compared to WT acinar cells. Scale bars 2µm.

Supplementary Figure 5

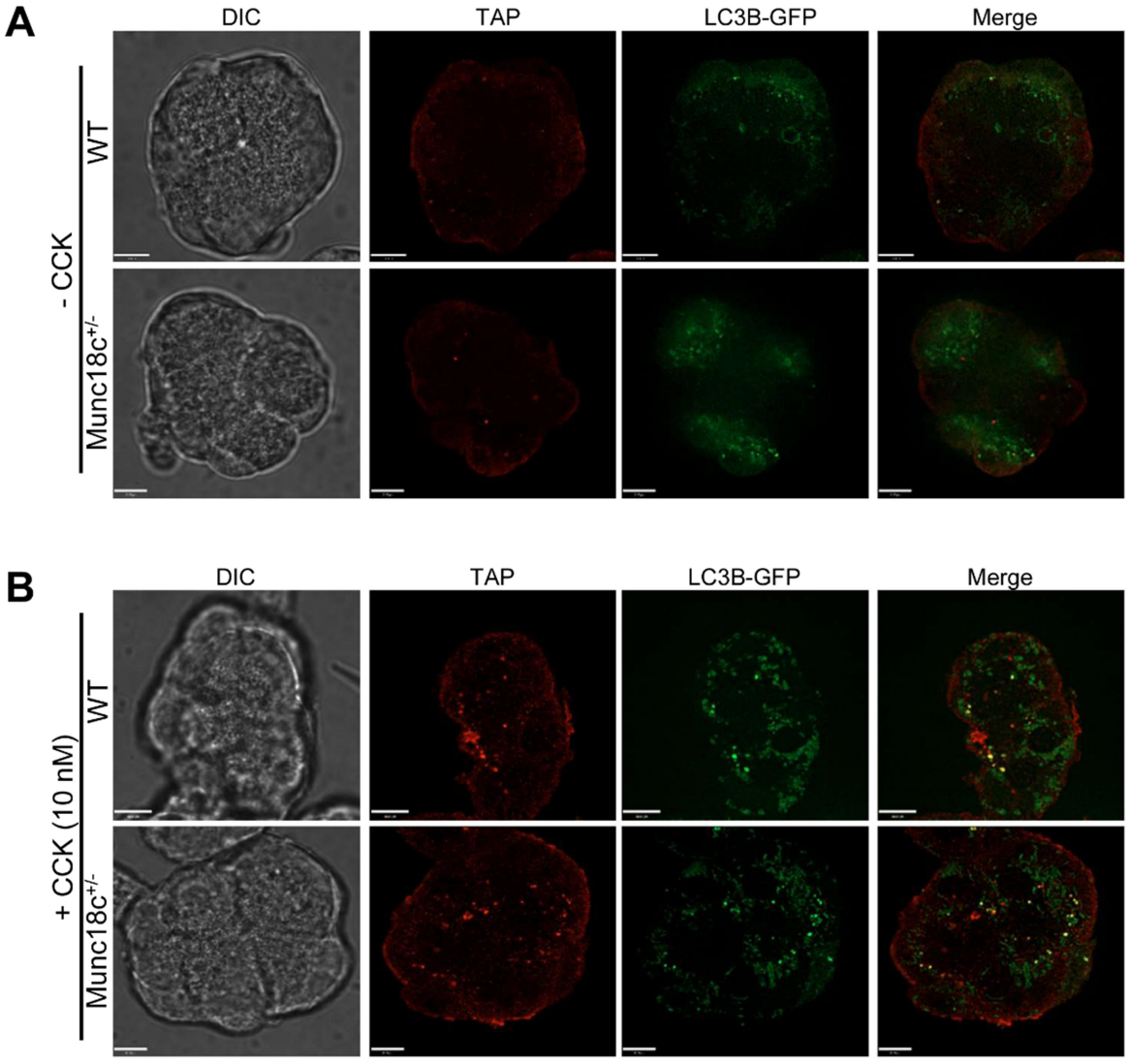

C

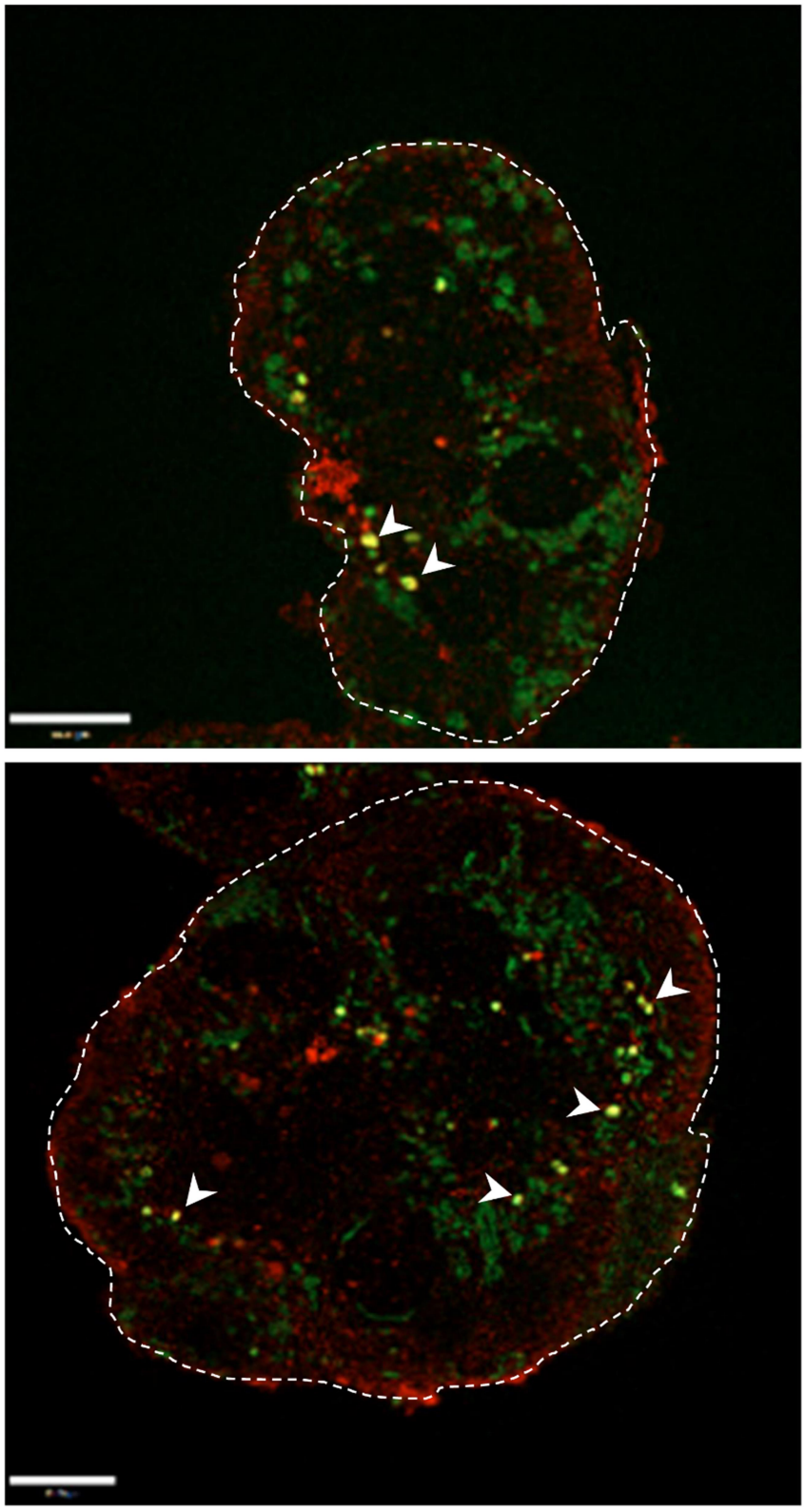

Supplementary Figure 5. Complete sequences of confocal immunofluorescence images of **(A)** LC3BGFP/TAP that correspond to **Fig. 6A**. (*A*) Corresponds to *top* panels of **Fig. 6A**, while (*B*) corresponds to *bottom* panels of **Fig. 6A**. In unstimulated acini in (A), there was very little TAP activity (*red* hotspots) and reduced number of LC3B vesicles (*green* hotspots), both of which increased after 10 nM CCK-8 stimulation (in B). (*C*) Enlargement of the Merge images in (B) showing more clearly their colocalization within the yellow hotspots (TAP activity within LC3B vesicles indicative of ALs, pointed by *white arrowheads*), which were more abundant in the Munc18c$^{+/-}$ than WT mouse acini. Scale bars 10 μm.